1 **Freshening of Antarctic Intermediate Water in the South Atlantic Ocean in 2005 - 2014**

2 Wenjun Yao [1], Jiuxin Shi[1], Xiaolong Zhao[2]

3 [1]Physical Oceanography Laboratory/CIMST, Ocean University of China and Qingdao

4 National Laboratory for Marine Science and Technology, Qingdao, China.

5 [2] North China Sea Marine Forecasting Center, State Oceanic Administration, Qingdao,

6 266061, Shandong, China

7 *Correspondence to:* Wenjun Yao (wjimyao@gmail.com)

8 **Abstract**

9 Basin-scale freshening of Antarctic Intermediate Water (AAIW) is reported to have

10 occurred in the South Atlantic Ocean during the period from 2005 to 2014, as shown by the

11 gridded monthly means Array for Real-time Geostrophic Oceanography (Argo) data. This

12 phenomenon was also revealed by two repeated transects along a section at 30° S, performed

13 during the World Ocean Circulation Experiment Hydrographic Program. Freshening of the

14 AAIW was compensated by a salinity increase of thermocline water, indicating a hydrological

15 cycle intensification. This was supported by the precipitation less evaporation change in the

16 Southern Hemisphere from 2000 to 2014. Freshwater input from atmosphere to ocean surface

17 increased in the subpolar high-precipitation region and *vice versa* in the subtropical

18 high-evaporation region. Against the background of hydrological cycle changes, a decrease in

19 the transport of Agulhas Leakage (AL) which was revealed by the simulated velocity field,

20 was proposed to be a contributor to the associated freshening of AAIW. Further calculation

21 showed that such decrease could account for approximately 53% of the observed freshening

22 (mean salinity reduction of about 0.012 over the AAIW layer). The estimated variability of

23 AL was inferred from a weakening of wind stress over the South Indian Ocean since the

24 beginning of the 2000s, which would facilitate freshwater input from the source region. The

25 mechanical analysis of wind data here was qualitative, but it is contended that this study

26 would be helpful to validate and test predictably coupled sea-air model simulations.

27 Keywords: Freshening; Antarctic Intermediate Water; South Atlantic; Agulhas Leakage;

28 Wind Stress

# 1   Introduction

Thermocline and intermediate waters play an important part in global overturning circulation by ventilating the subtropical gyres in different parts of the world oceans [*Sloyan and Rintoul*, 2001]. They also constitute the northern limb of the Southern Hemisphere supergyre [*Ridgway and Dunn*, 2007; *Speich et al.*, 2002].

Previous studies have addressed the variability of intermediate water. *Wong et al.* [2001] found that the intermediate water had freshened between the 1960s and the period 1985-94 in the Pacific Ocean. *Bindoff and McDougall* [2000] reported that there had been freshening of water between 500 and 1500 db from 1962 to 1987 along 32° S in the Indian Ocean. *Curry et al.* [2003] showed a salinity reduction on the isopycnal surface of intermediate water for the period 1950s - 1990s in the western Atlantic. The freshening variability can be traced back to the signature of water in the formation regions [*Church et al.*, 1991]. The freshening examples given above are in agreement with the enhancement of the hydrological cycle, in which the wet (precipitation ($P$) > evaporation ($E$), $P$ dominance) subpolar regions have been getting wetter and vice versa for the dry ($E$ dominance) subtropical regions over the last 50 years [*Held and Soden*, 2006; *Skliris et al.*, 2014].

Antarctic Intermediate Water (AAIW) is characterized by a salinity minimum (core of AAIW) centered at the depths of 600 m and 1000 m (Fig. 1), which lies within the potential density (reference to sea surface) range of $\sigma_0$ = 27.1 - 27.3 kg/m$^3$ [*Piola and Georgi*, 1982]. The AAIW is found from just north of the Subantarctic Front (SAF) [*Orsi et al.*, 1995] in the Southern Ocean and can be traced as far as 20° N [*Talley*, 1996]. It is generally accepted that the variability of AAIW is largely controlled by air-sea-ice interaction [*Close et al.*, 2013; *Naveira Garabato et al.*, 2009; *Santoso and England*, 2004], but the argument about its origin and formation process continues. For example, there is the circumpolar formation theory of AAIW along the SAF, through mixing with Antarctic Surface Water (AASW) along isopycnals [*Fetter et al.*, 2010; *Sverdrup et al.*, 1942]. Alternatively, it has been proposed that there is a local formation of AAIW in specific regions, as a bi-product of Subantarctic Mode

56  Water (SAMW) relating to deep convection [*McCartney*, 1982; *Piola and Georgi*, 1982]. The

57  first standpoint states that the AAIW are primarily derived from entirely subpolar sources,

58  meanwhile the second one emphasizes the role that air-sea interaction plays in the oceans

59  south of South America.

60      In the South Atlantic, AAIW constitutes the return branch of the Meridional Overturning

61  Circulation (MOC) [*Donners and Drijfhout*, 2004; *Speich et al.*, 2007; *Talley*, 2013]. As an

62  open ocean basin, the South Atlantic is fed by two different sources of AAIW [*Sun and Watts*,

63  2002]. The first is younger, fresher and has a lower apparent oxygen utilization (AOU) and

64  originates from the Southeast Pacific [*McCartney*, 1977; *Talley*, 1996] and the winter waters

65  west of the Antarctic Peninsula [*Naveira Garabato et al.*, 2009; *Santoso and England*, 2004].

66  These source regions of AAIW are mostly dominated by the net surface freshwater flux from

67  atmosphere to ocean (*P>E*), which facilitates the freshening of AAIW with time. The second

68  is the older, saltier and higher AOU AAIW which comes from the Indian Ocean transported

69  by the Agulhas Leakage (AL) as Agulhas rings (Fig. 2). The mixture of the above two types

70  of AAIW can lead to a transition of hydrographic properties across the subtropical South

71  Atlantic [*Boebel et al.*, 1997].

72      The influence of AL on the variability of AAIW in the South Atlantic has been

73  demonstrated to be substantial [*Hummels et al.*, 2015; *Schmidtko and Johnson*, 2012], as 50 -

74  60% of the Atlantic AAIW originates from the Indian Ocean [*Gordon et al.*, 1992; *McCarthy*

75  *et al.*, 2012], with increased (decreased) transport of AL relating to salinification (freshening)

76  of AAIW. AL has apparently increased during the period from the 1950s to the early 2000s

77  [*Durgadoo et al.*, 2013; *Lübbecke et al.*, 2015], but there have been no studies addressing the

78  influence of AL on the AAIW in South Atlantic since 2000.

79      With the instigation of the Array for Real-time Geostrophic Oceanography (Argo)

80  program, *in-situ* hydrographic observation has tremendously expanded since 2003 [*Roemmich*

81  *et al.*, 2015], particularly in the Southern Ocean (SO) where historical data are sparse and

82  intermittent. This decreases the uncertainty of estimates for the research on both seasonal and

83  decadal variations of subsurface and intermediate waters.

84      The present work reports the freshening of AAIW in the South Atlantic over the

85    preceding decade (2005 - 2014) using gridded monthly data based on Argo data. Against the

86    background of an enhanced hydrological cycle, decreased transport of AL contributed to such

87    freshening and may be driven by a weakening of wind stress in the South Indian Ocean

88    during the same period.

89    **2    Data and methods**

90      Based on individual temperature ($T$) and salinity ($S$) profiles from Argo, International

91    Pacific Research Centre (IPRC) gridded monthly means data for the period 2005-2014 have

92    been produced using variational interpolation. The IPRC data have 27 levels from 0 to 2000

93    m depth vertically, nominal 1°×1° grid globally and monthly temporal resolution

94    (http://apdrc.soest.hawaii.edu/projects/Argo/data/gridded/On_standard_levels/index-1.html).

95    To reduce the error from low vertical resolution of data when computing the hydrographic

96    values on isopycnal surfaces, $T$ and $S$ profiles were first interpolated onto 1 m vertical depth

97    intervals using a spline method in the intermediate water depth, and a linear method in the

98    thermocline depth. Because the IPRC data were interpolated from randomly distributed Argo

99    profiles, it is necessary to demonstrate the robust nature of their signals by comparing them

100    with the other Argo gridded products. As a result, the Japan Agency of Marine-Earth Science

101    and Technology (JAMSTEC, [*Hosoda et al.*, 2008]) $T$ and $S$ data from 2005 to 2014 with 1°

102    longitude and 1° latitude resolution were also collected for comparison and verification. The

103    number of Argo profiles is rapidly increasing year by year, and part of their distribution has

104    been outlined in previous studies, *inter alia Hosoda et al.* [2008] and *Roemmich et al.* [2015].

105      Two hydrographic cruises of repeated transects along 30° S were conducted during the

106    World Ocean Circulation Experiment (WOCE) Hydrographic Program

107    (http://www.nodc.noaa.gov/woce/wdiu/diu_summaries/whp/index.htm). Their locations are

108    presented in Fig. 2. The first transect consisted of 72 stations in 2003 by the R/V Mirai (Japan,

109    [*Kawano et al.*, 2004]), the second was in 2011 with 81 stations sampled from the Ronald H.

110    Brown (United States, [*Feely et al.*, 2011]). These two transects not only occupied almost

111 identical station positions in the subtropical South Atlantic, but also conducted in the same

112 season (November and October respectively). Furthermore, the time interval between the two

113 sections from Nov 2003 to Oct 2011 is very similar to the period covered by the IPRC data

114 (Jan 2005 - Dec 2014) and can therefore be used to validate those results.

115 To smooth out some of the higher frequency variability (i.e. mesoscale eddies and

116 internal waves), the investigation of halocline variation should be along neutral density

117 surfaces [*McCarthy et al.*, 2011; *McDougall*, 1987]. The layer of AAIW is defined using

118 neutral density ($\gamma^n$, unit: kg/m$^3$) [*Jackett and McDougall*, 1997] instead of potential density,

119 with the upper and lower boundaries being $27.1\gamma^n$ and $27.6\gamma^n$ [*Goes et al.*, 2014], respectively.

120 Monthly 10 m wind fields between years 1980 and 2014 from the ERA-Interim archive

121 at the European Centre for Medium Range Weather Forecasts (ECMWF)

122 (http://apps.ecmwf.int/datasets/data/interim-full-daily/levtype=sfc/) were used to investigate

123 the decadal variability of wind stress (WS) over the South Indian Ocean. Another reanalysis

124 wind product of National Centers for Environmental Prediction-Department of Energy

125 Atmospheric Model Intercomparison Project reanalysis 2 (NCEP2,

126 http://www.esrl.noaa.gov/psd/data/gridded/data.ncep.reanalysis2.html) was also used for the

127 period 1980-2014. Additionally, the satellite-derived wind products of the Quick

128 Scatterometer (QuikSCAT) for 2000-2007 and the Advanced Scatterometer (ASCAT) for

129 2008-2014 (both in ftp://ftp.ifremer.fr/ifremer/cersat/products/gridded/MWF/L3/) were used

130 to compare and verify the decadal variability of WS revealed by the ERA-Interim wind

131 product. In this work, the WS over open ocean was calculated from 10 m wind field data

132 using the equation adopted in *Trenberth et al.* [1989].

133 Reanalysis data including precipitation (*P*) and evaporation (*E*) from the ERA-Interim

134 were used to reveal the freshwater input from the atmosphere to the ocean surface in the

135 preceding decade.

136 The Simple Ocean Data Assimilation version 3.3.1 (SODA3.3.1,

137 http://www.atmos.umd.edu/~ocean/), which is forced by the Modern-Era Retrospective

138 Analysis for Research and Applications Version 2 (MERRA2), spans the 36-year period

139 1980-2015 ([*Carton et al.*, 2016]). The global simulated velocity field at specified depths

140 provided by SODA makes it possible to evaluate the transport of AL.

## 141 3 Freshening of Antarctic Intermediate Water

### 142 3.1 Freshening observed from Argo gridded products

143 The Argo gridded products provide a globally distributed and continuous time series of $T$

144 and $S$ profiles down to 2000 m ocean depth. The present work focused on the AAIW in the

145 South Atlantic Basin (Fig. 2, Region A), which encompasses most of the subtropical gyre and

146 a part of the tropical regimes [*Boebel et al.*, 1997; *Talley*, 1996]. Computed from the Argo

147 gridded data of IPRC, the biennial mean $\theta$-$S$ diagram (Fig. 3a) clearly shows that the AAIW

148 has experienced a process of progressive basin-scale freshening during the period from Jan

149 2005 to Dec 2014. The linear trend of salinity (Fig. 3b) further reveals that the freshening

150 takes up most of the AAIW layer but with a little salinification in the deeper part. Except

151 around the $27.42\gamma^n$ neutral density surface, the AAIW variation is significant at the 95%

152 confidence level, using the $F$-test criteria. In comparison with Fig. 3a, it was found that the

153 cut-off point of transformation from salinity decrease to increase is near the salinity minimum.

154 Above the salinity minimum, the shift of $\theta$-$S$ trends towards cooler and fresher values along

155 density surfaces and seem to be a response to the warming and freshening of surface waters

156 where AAIW ventilates. Such thermohaline change has also been found in the Pacific and

157 Indian oceans over a different time period [*Wong et al.*, 1999]. *Church et al.* [1991] and

158 *Bindoff and Mcdougall* [1994] have researched the counterintuitive cooling of AAIW

159 temperature induced by warming of surface water. They showed that a warming parcel in the

160 mixed layer would subduct further equatorward, which would lead the $\theta$-$S$ curve to become

161 cooler and fresher at a given density. The salinity decrease of the AAIW core indicates that

162 such change can only be induced by freshwater input from the source region, as mixing with

163 more saline surrounding waters cannot give rise to a salt loss in the salinity minimum layer.

164        To demonstrate the robustness of AAIW variations revealed by the IPRC data, re-plots

165        of Fig. 3a-b using another Argo gridded product from JAMSTEC, are also shown for

166        comparison (see Supplementary 1, only the AAIW layer shown). Not only was the same

167        variation along density surfaces in the AAIW layer found, but also a freshening of the salinity

168        minimum. The isoneutral salinity increases of both IPRC and JAMSTEC data below the

169        salinity minimum are quite small. The main discrepancy between them is that the salinity

170        reduction in the JAMSTEC data is somewhat less than IPRC and at a higher 95% confidence

171        level (a mean of 0.006 between $27.1\gamma^n$ and $27.6\gamma^n$).

172        The freshwater gain for the basin-scale salinity decrease of AAIW (mean salinity

173        difference of 0.012 between $27.1\gamma^n$ and $27.6\gamma^n$ over a mean water mass thickness of 500 m) is

174        estimated at 17mm $yr^{-1}$ in its source region. This assumes that the South Atlantic only

175        experienced freshwater input and nothing changed, thus the relationship between the salinity

176        in 2005 and 2014 per unit area was roughly $S_{2005}*500 = S_{2014}*(500+\Delta d)$. Here $S_{2005} =$

177        $S_{2014}+0.012$ and $\Delta d$ is the freshwater gain during the covered period. However, the

178        depth-integrated salinity change over the water column (between $26.6\gamma^n$ and $27.6\gamma^n$) was

179        0.0014, since a salinity increase of thermocline water balances the observed freshening of

180        AAIW. This salinity budget implies contemporary hydrological cycle intensification in the

181        southern hemisphere, which is illustrated by the *P* minus *E* change from 2000 to 2014, with

182        *P-E* increasing in the subpolar region and *vice versa* in the subtropical region (Fig. 4a). In

183        these cases, the thermocline (intermediate) water that ventilates in the high-evaporation

184        (precipitation) subtropical (subpolar) regions gets more saline (freshened), as shown by the

185        hydrographic observations (Fig. 3b).

186        Against the background of hydrological cycle augmentation, the annual freshwater input

187        in the AAIW ventilation region during the freshening period increased by 0.02 mm $day^{-1}$,

188        about 17% of the *P-E* in 2005 (Fig. 4b). It is considered that the significant *P-E* increase

189        began around 2003 (Fig. 4b, 5-yr running mean line), which means the observed freshened

190        AAIW could be traced back to 2003. Though it was not possible to compute the direct

191        freshwater input to the South Atlantic Basin in this study, the Argo era freshening of AAIW is

192        qualitatively consistent with the freshwater gain in its source region.

### 3.2 Freshening in the quasi-synchronous WOCE CTD observations

Here two synoptic transatlantic sections from WOCE hydrographic program were used to explore the decadal freshening signal identified in the above subsection. Similar to Fig. 3a, the sectional mean $\theta$-$S$ diagram (Fig. 5a) displays the same shift of thermohaline values, including freshening of the salinity minimum, salinity reduction in the upper AAIW layer and *vice versa* in the lower layer. Compared to the $\theta$-$S$ curves of IPRC data (Fig. 3a), the curves of WOCE (Fig. 5a) seem to be, in general, cooler $\theta$ and fresher $S$. It is suggested that this is because the IPRC mean is weighted towards the warmer and saltier waters in the north.

Unlike the Argo gridded product which has a continuous time series of $T$ and $S$ data, there are only two sections in the WOCE observations. Instead of calculating the linear trend of salinity (as was done with the IPRC data), the difference of salinity observed in 2003 and 2011 was estimated (Fig. 5b). The light grey shading denotes the 95% confidence interval using simple $t$-test criteria and considering the number of degrees of freedom. Above the salinity minimum, the freshening of AAIW revealed by the IPRC and the WOCE data are quite similar, with the maximum appearing near $27.2\gamma^n$. Because the last WOCE observation terminated in 2011 and the salinity reduction would continue at least up to 2014 as displayed in Fig. 3a, the magnitude of the freshening in WOCE (Fig. 5b) is smaller than IPRC (Fig. 3b). In the water layer below the salinity minimum (around $27.41\gamma^n$), the salinity increase shown in the WOCE data is relatively large (Fig. 5b). This is thought to be because the salinity rise reached its maximum around 2011, which is shown in the time series of basinwide averaged salinity on $27.45\gamma^n$ and $27.55\gamma^n$ density surfaces (see Supplementary 2).

For the salinification of thermocline water, there is a large discrepancy between IPRC and WOCE data on neutral density surfaces $26.6$-$26.7\gamma^n$ (Fig. 5b). It is considered that this would not affect the salinity budget over the water column (Fig. 5b), given that the salt gain of thermocline water would balance the observed freshened AAIW. In conclusion, the general trend and consistency of the detail therein of the salinity change over the last ten-year time period revealed by the IPRC and the WOCE data, leads us to state that the freshening of AAIW is a robust finding and valid.

## 4    Decrease of Agulhas Leakage transport

AAIW in the South Atlantic is largely influenced by the AL through the intermittent pinching off of Agulhas rings (Fig. 2) [*Beal et al.*, 2011], transferring salty thermocline and intermediate water from the Indian Ocean to the South Atlantic [*De Ruijter et al.*, 1999]. The above discussion suggests that the freshening of AAIW was induced by the input of freshwater from the source regions, which consist of the southeast Pacific Ocean and the circumpolarly subpolar oceans (see introduction). As a result, if the transport of more saline water from the Indian Ocean decreased, it would promote the effect of this freshwater increase. In this section, the decrease of AL transport was evaluated by depth integration of velocity field and further demonstrated by using an indirect indicator.

### 4.1    Evaluation from SODA velocity

In modeling studies, it is widely accepted to quantify the leakage using a Lagrangian approach [*Biastoch et al.*, 2009; *van Sebille et al.*, 2009]. Here a simplified strategy was employed to compute the leakage by integrating the velocity within AAIW layer (approximately between 610 and 1150m, according to Fig. 1), which was shown to result in a similar quantification to the Lagrangian one [*Le Bars et al.*, 2014]. The depth integration is along the Good hope section (green line in Fig. 2), using the cross-component velocity. Note that the leakage calculation is from the continent to the zero line of the barotropic streamfunction, which is the separation of the Agulhas regime and the Antarctic Circumpolar Current [*Biastoch et al.*, 2015].

Before showing the transport computed from the SODA velocity data, it is necessary to verify that the SODA hydrographic data show the same freshening of AAIW as other datasets. AAIW in the South Atlantic was also found to have freshened during period 2005-2014, though with relatively small magnitude (Supplementary 3). Yearly leakage computation within the AAIW layer was carried out for the period 2000-2015 (Fig. 6). It shows that the leakage in the early 2010s is smaller than that in the middle and late 2000s, forming a

247 decreasing trend in a nearly ten-year period. This estimation of leakage seems to be consistent

248 with the indirect estimate of AL transport given below.

249     The following calculation is to simply estimate the contribution of the AL transport

250 change to our observed freshening. As shown by Fig. 6, the decreased rate of AL transport

251 could be taken to be 2 Sv in a ten-year time period, assuming that this rate increased year by

252 year in the study period (i.e., 0.2 Sv in the first year, 0.4 Sv in the second year, and so on).

253 According to *Sun and Watts* [2002], here we take the salinity difference of $\Delta S$=0.1 between

254 the South Indian and the South Atlantic in the AAIW layers. The other parameters, including

255 total seconds in a year, water thickness of the AAIW layer, the area of Region A, are taken to

256 be $\Delta t$=365×24×3600s, $\Delta d$=500 m and $\Delta s_A$=1.09×10$^{13}$ m$^2$, respectively. Therefore, the salinity

257 decrease from 2005 to 2014 induced by the change of AL transport, should be

258 (0.2+0.4+…+2)×10$^6$×$\Delta t$×$\Delta S$/($\Delta s_A$×$\Delta d$). This results in a salinity reduction of 0.0064, which

259 could account for approximately 53.0% of the observed freshening revealed by the IPRC data.

260 Though our estimate here is quite rough, we can state that, during 2005-2014, the AL

261 significantly influenced the salinity change in the South Atlantic Ocean within the AAIW

262 layers.

263 **4.2    Weakening of the westerlies in the South Indian Ocean**

264     Continuous measurements of the AL transport have never been realized so far. An

265 earlier study suggested that an increased AL transport correlates well with a poleward shift of

266 the westerly winds [*Beal et al.*, 2011]. However, after using reanalysis and climate models,

267 *Swart and Fyfe* [2012] argued that the strengthening of Southern Hemisphere surface

268 westerlies has occurred without major transgressions in its latitudinal position over the period

269 1979-2010, during which period the AL has largely increased [*Biastoch et al.*, 2009]. A more

270 recent study of *Durgadoo et al.* [2013] showed that the increase of AL is concomitant with an

271 equatorward rather than a poleward shift of westerlies in their simulation cases. They also

272 concluded that the intensity of westerlies is predominantly responsible in controlling this

273 Indian-Atlantic transport. Many relevant studies agreed on this relationship, that the

274 enhancement of westerly wind intensity is related to the increase of AL [*Goes et al.*, 2014;

275 *Lee et al.*, 2011; *Loveday et al.*, 2015].

276      The AL corresponds most significantly to westerly wind strength averaged over the

277 Indian Ocean in contrast to that averaged circumpolarly or locally [*Durgadoo et al.*, 2013].

278 According to the work of *Durgadoo et al.* [2013], zonally averaged WS was calculated from

279 the ERA-Interim wind product over the Indian Ocean (20-110° E) for every 5-yr period since

280 1980 (Fig. 7a and d). Previous studies [*Lee et al.*, 2011; *Loveday et al.*, 2015] have found that

281 the WS has increased considerably from 1980s to the beginning of 2000s (Fig. 7d), consistent

282 with the contemporary increase of AL transport. Though there are oscillations during 1990s,

283 the WS reached its peak around the years 2000-2004 (Fig. 7d), then began to decline. It can

284 be concluded that the WS has weakened for period 2000 – 2014 (Fig. 7d), which implies a

285 concurrent decrease of AL transport.

286      In addition to the ERA-Interim wind data, we have further checked the zonally averaged

287 WS over the Indian Ocean (20-110° E), using another reanalysis product of NCEP2 (Fig. 7b

288 and e) and the combined QuikSCAT-ASCAT (Fig. 7c and f) satellite-derived wind products.

289 The three zonally averaged WS agree that during the period 2000-2014, the westerlies

290 reached a peak in the years 2000-2004, and then progressively subsided through 2005-2009 to

291 2010-2014. The process of gradual decline of WS is most pronounced in the NCEP2 data. It

292 is noteworthy that none of the three products show a significant meridional shift of the

293 latitude of maximum WS from 2000 to 2014, in corroboration with the conclusion of *Swart*

294 *and Fyfe* [2012].

295 **4.3    Evidence from other works**

296      Many efforts have been made to estimate AL transport, especially using model

297 simulations [*Lübbecke et al.*, 2015; *Loveday et al.*, 2015]. In recent years, *Le Bars et al.* [2014]

298 provided the time series of AL transport over the satellite altimeter era, computed from

299 absolute dynamic topography data, which can show the decadal variation of AL present. In

300 their result (Figure 8 in *Le Bars et al.* [2014]), the anomalies of AL from satellite altimetry

301 reached a peak around 2003 (annual average), and then began to subside, apart from a

302 mid-2011 increase. In addition, their negative trend of AL (Figure 9 in *Le Bars et al.* [2014])

303 over the period from Oct 1992 to Dec 2012 indicates that the transport was reduced during the

304 2000s in contrast to the 1990s. Another study by *Biastoch et al.* [2015] should be of help in

305 the present discussion. Though the time series of AL obtained from models didn't show a

306 distinct decline of AL transport in the last decade, which seems partly due to the data filter

307 applied and the end of the time series (Figure 4 in *Biastoch et al.* [2015]), it displays a

308 maximum of salt transport around 2000 (Figure 5 in *Biastoch et al.* [2015]). This peak and the

309 subsequent decline of salt transport are consistent with the freshening of AAIW over the

310 similar time period considered here.

311      Thus, in addition to the freshwater input that gave rise to the salt loss of the AAIW in the

312 South Atlantic Ocean, reduced transport of AL or salt would further enhance this signal.

313 Unfortunately, the analyses of the contributions from both the source region and the AL were

314 only quantitative. Future work should be focused on quantification of each factor based on

315 model simulations.

316

317 **5     Conclusions and discussions**

318      The analysis of IPRC gridded data shows that the AAIW in the South Atlantic has

319 experienced basin-scale freshening for the period from Jan 2005 to Dec 2014 (Fig. 3a and b),

320 with freshwater input estimated at 17 mm yr$^{-1}$ in its source region. Two transects of WOCE

321 hydrographic program observed in 2003 and 2011 also reveal the above variation of AAIW in

322 the last decade (Fig. 3c and d).

323      This freshening in the intermediate water layer is thought to be compensated by

324 increased salinity in shallower thermocline water, indicating a contemporary intensification of

325 hydrological cycle (Fig. 3b and Fig. 5b). In this case the freshwater input from atmosphere to

326 ocean surface increased in the subpolar high-precipitation region and *vice versa* in the

327 subtropical high-evaporation region (Fig. 4a). Over the last ten-year time period, significant

328    freshwater gain began around 2003 (Fig. 4b), suggesting the observed freshened AAIW could

329    be traced back to this time.

330        Against the background of hydrological cycle intensification, the decrease of AL

331    transport is proposed to contribute to the freshening of AAIW in the South Atlantic,

332    associated with a weakening of westerlies over the South Indian Ocean. This decrease was

333    revealed by the leakage evaluation along the Good Hope section. The mechanical analysis

334    shows that the WS over the South Indian Ocean reached its peak around 2000-2004 and

335    began to subside through 2005-2009 to 2010-2014 (Fig. 7), reversing its increasing phase

336    from 1950s to the beginning of 2000s, during which period the AL had increased [*Durgadoo*

337    *et al.*, 2013; *Lübbecke et al.*, 2015]. This indirectly estimated variability of AL is consistent

338    with other studies covering a similar period [*Biastoch et al.*, 2015; *Le Bars et al.*, 2014]. As

339    the AAIW carried by the AL is more saline relative to its counterpart in the South Atlantic

340    Ocean, its decrease would promote the effect of freshwater input from the source region. Our

341    estimate further suggests that such an induced freshwater input by AL could account for

342    approximately 53% of the observed freshening.

343        One might ask if there are any other sources that could significantly affect the AAIW in

344    the South Atlantic Ocean, for example the Southeast Pacific (see Introduction). To clarify this

345    question, we displayed the EOF1 pattern and its time series (called the principal components)

346    of salinity on the $27.36\gamma^n$ (around $27.2\sigma_0$) surface (Fig. 8) in the Southern Hemisphere, which

347    explains 55.4% of the variance. It shows that in 2000-2014, the most significant salinity

348    reduction appeared in the South Indian Ocean, especially in the region of Agulhas Current

349    System. It also shows that compared to the West Atlantic, the East Atlantic experienced the

350    major salinity reduction, whose intermediate water is largely fed by its counterpart in the

351    South Indian Ocean. In addition to these salinity changes, we also note that the salinity

352    decrease in the Southeast Pacific was considerably less than that in the South Indian and the

353    South Atlantic. Therefore, it implies that the Southeast Pacific did not play an important role

354    in our observed AAIW freshening.

355        The purpose of this work is to reveal the decadal freshening of AAIW in the South

356    Atlantic Ocean over the last ten-year time period, and suggest the related contributing

357 mechanism. Future work should be focused on the quantification of these two contributors,

358 and the influence they have on the world ocean circulation, through modelling studies.

359

360    Acknowledgements
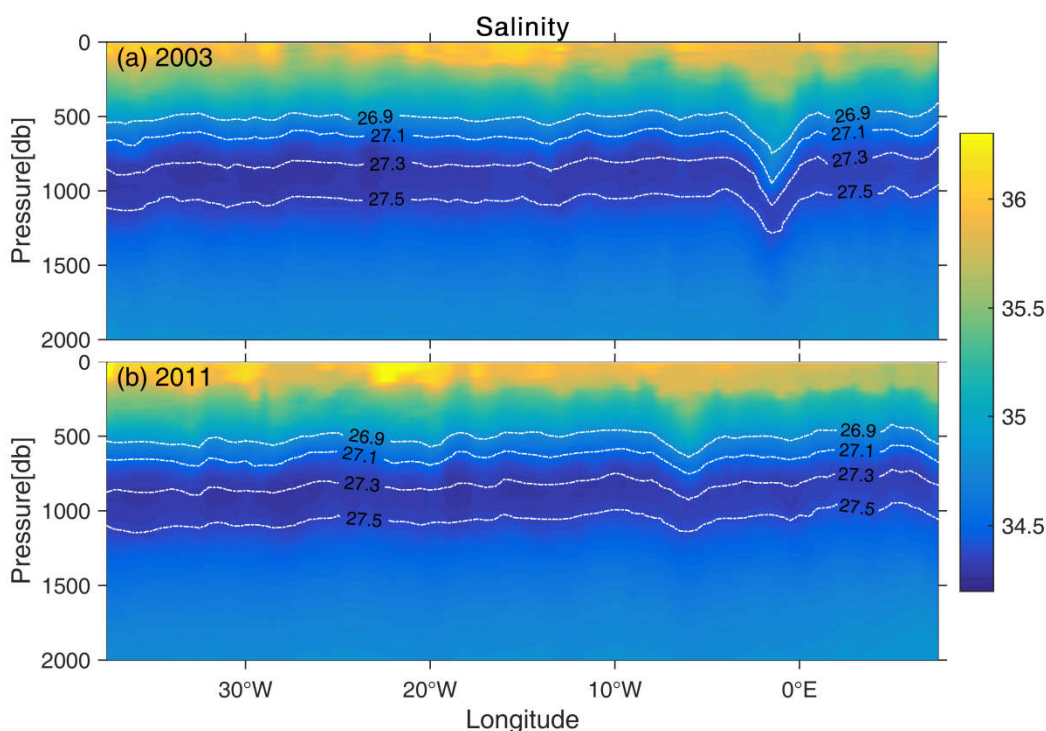
363

364    Captions of Figures



365

366 Fig. 1 WOCE salinity sections along 30° S in the South Atlantic Ocean (positions shown in

367 Fig. 2) observed in (a) 2003 and (b) 2011. Overlaid white solid-dotted lines are $\gamma^n$ surfaces

368 ranging from 26.9 to 27.5 kg/m$^3$, with 0.2 kg/m$^3$ interval.

369

370
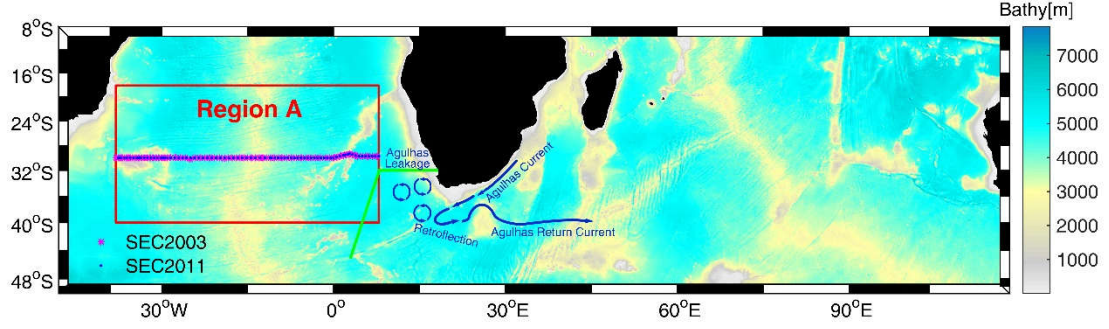
Fig. 2 Bathymetry of the South Indian-Atlantic oceans. Color shading is ocean depth. Red box delineates the area for the basinwide average of gridded data (hereafter refers to Region A). The green line shows the Good Hope section which is used to calculate the leakage transport to the South Atlantic. Magenta stars represent transatlantic CTD stations measured in 2003, meanwhile blue dots in 2011. The Agulhas Current, Retroflection, Agulhas Return Current and Agulhas Leakage (as eddies) are also shown and ticked.

377



378
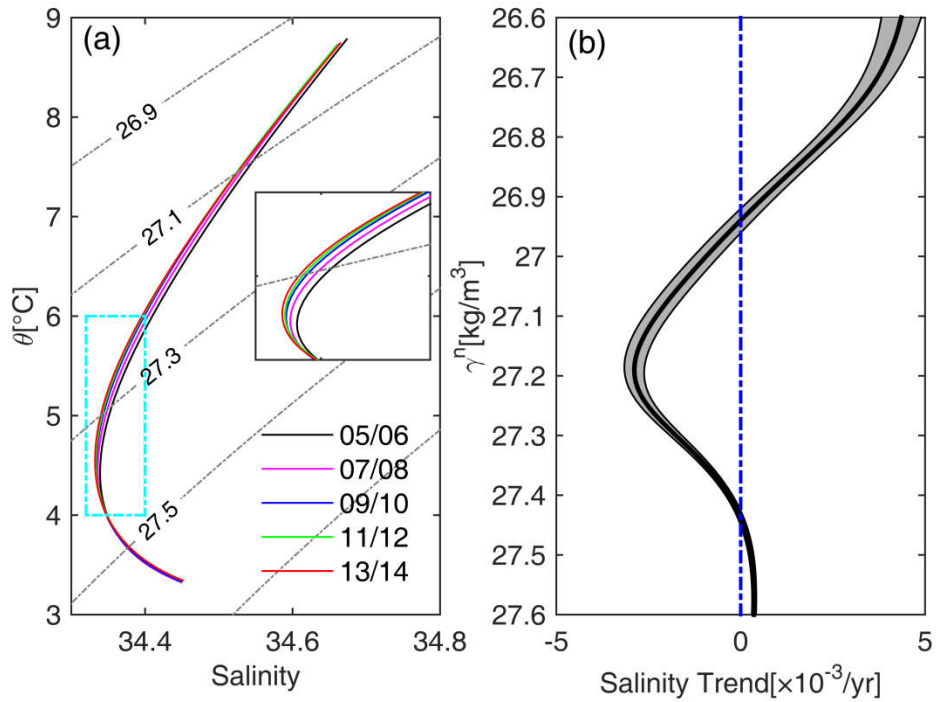
Fig. 3 (a) Biennial mean $\theta$-$S$ diagram averaged over Region A for IPRC data with $\gamma^n$ surfaces superimposed (grey solid-dotted lines). The inserted figure is the magnification of the area delineated by cyan solid-dotted box. The corresponding time for each $\theta$-$S$ curve is listed in their bottom-right corner (i.e. 05/06 for 2005-2006). (b) Salinity trend along $\gamma^n$ surfaces for period Jan 2005 - Dec 2014 is displayed by the thick black line, and the 95% confidence intervals ($F$-test) are represented by the light grey shadings, calculated from IPRC data.

385

386

387



388
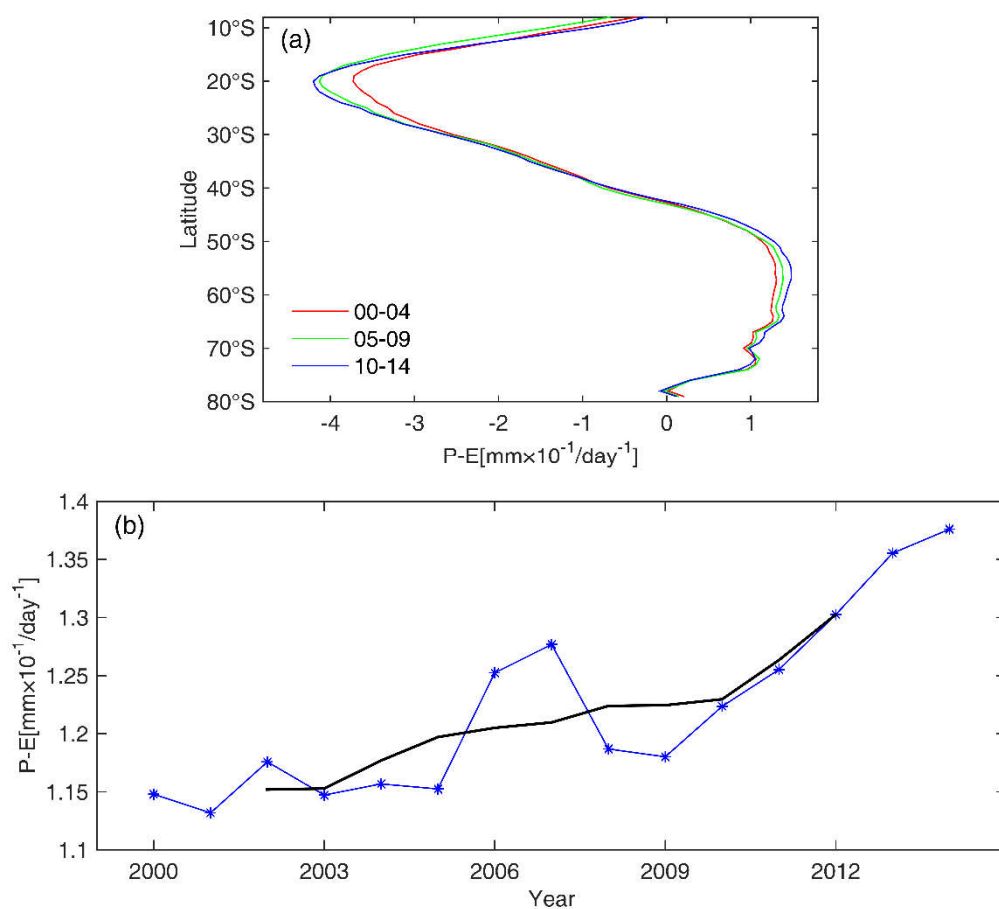
Fig. 4 Calculated from ERA-Interim precipitation and evaporation data: (a) Zonally mean (ocean areas only) of annually *P-E* (freshwater input, mm day$^{-1}$), each line represents a 5-yr averaged result. The corresponding time period (i.e. 00-04 for 2000-2004) is listed in the bottom-left corner. (b) Time series of annually *P-E* averaged over the oceans in 45-65° S, 0-360° E band from 2000 to 2014 (blue star), and its 5-yr running mean (black).

389
390
391
392
393
394
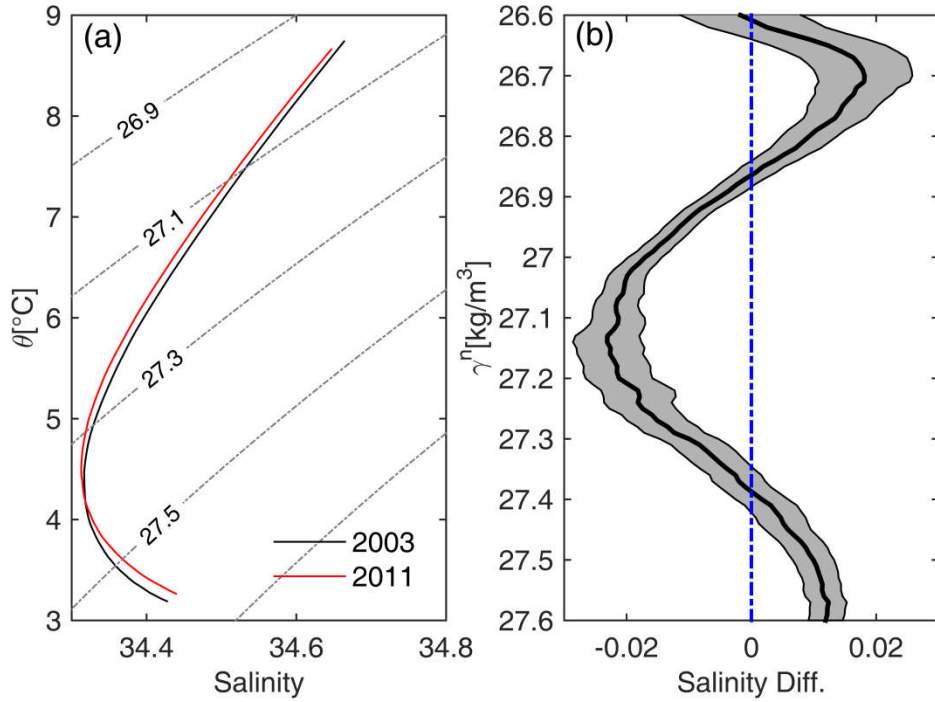
Fig. 5 (a) The same as Fig. 3a but for sectional mean of WOCE hydrographic casts. The corresponding year for each $\theta$-$S$ curve is listed in the bottom-right corner. (b) Sectional mean differences (thick black line) of WOCE hydrographic data along $\gamma^n$ and their 95% confidence intervals (grey shadings, $t$-test).
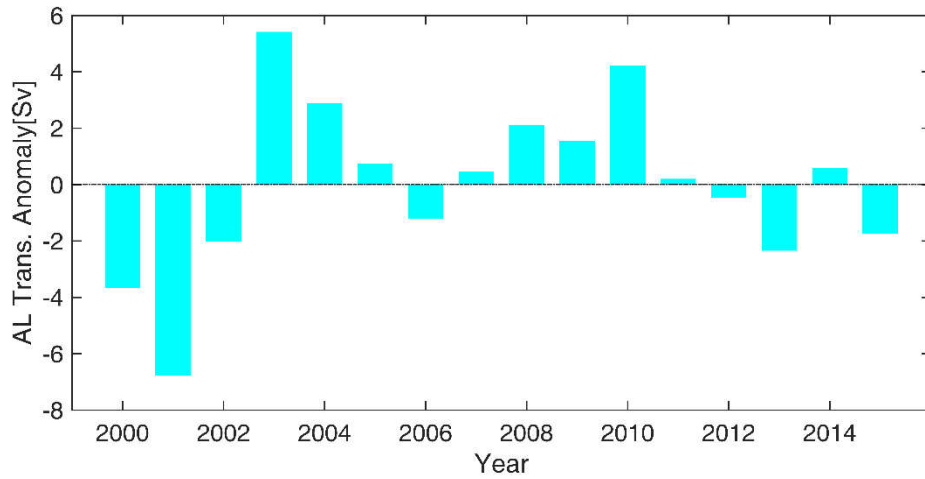


Fig. 6 Computation of Agulhas Leakage transport anomaly from the SODA velocity field along the Good Hope Line. Note that the depth integration is only for the AAIW layer.
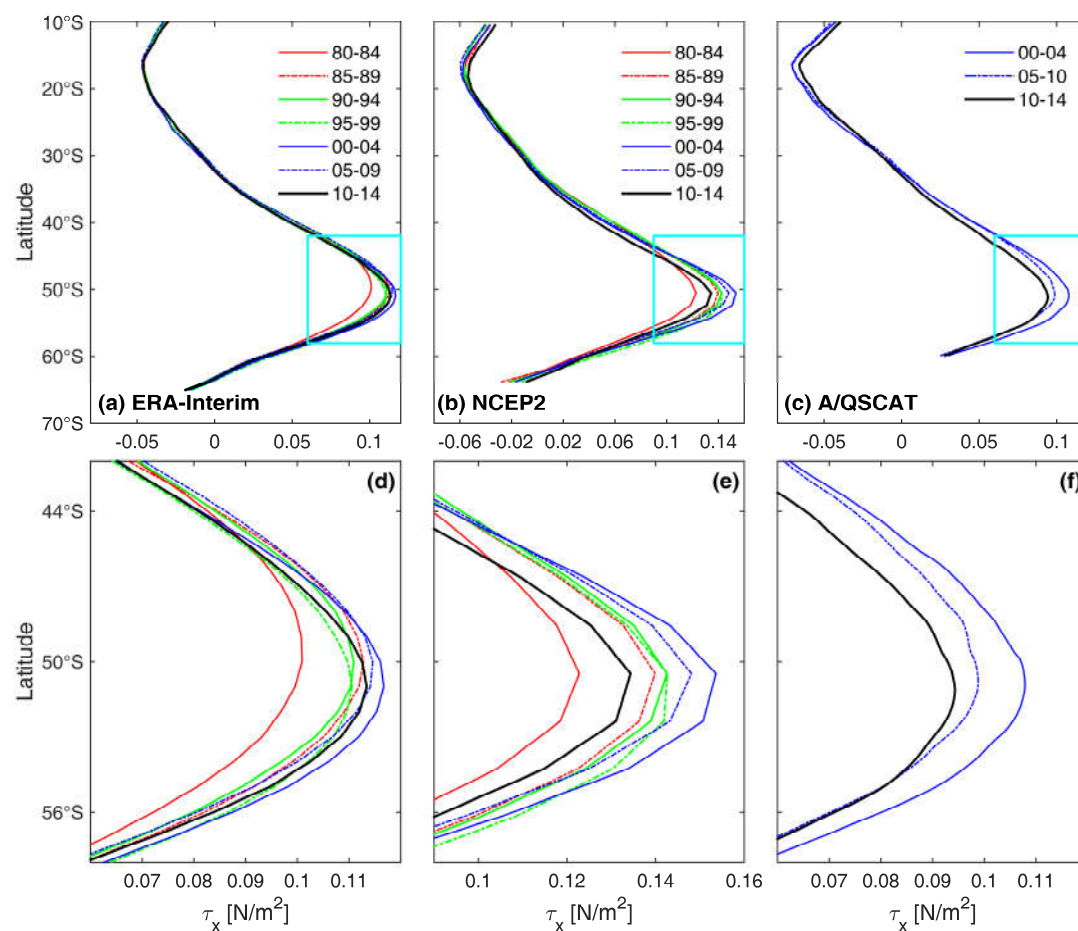
Fig. 7 Zonally averaged wind stress calculated from the wind product of (a) ERA-Interim, (b) NCEP2 and (c) ASCAT/QSCAT over the Indian Ocean (20 -110° E) for different periods (i.e. 80-84 for Jan 1980 - Dec 1984; 00-04 for Jan 2000 - Dec 2004) listed in the top-right corners. (d), (e) and (f) are the magnification of cyan boxes in (a), (b) and (c), respectively.
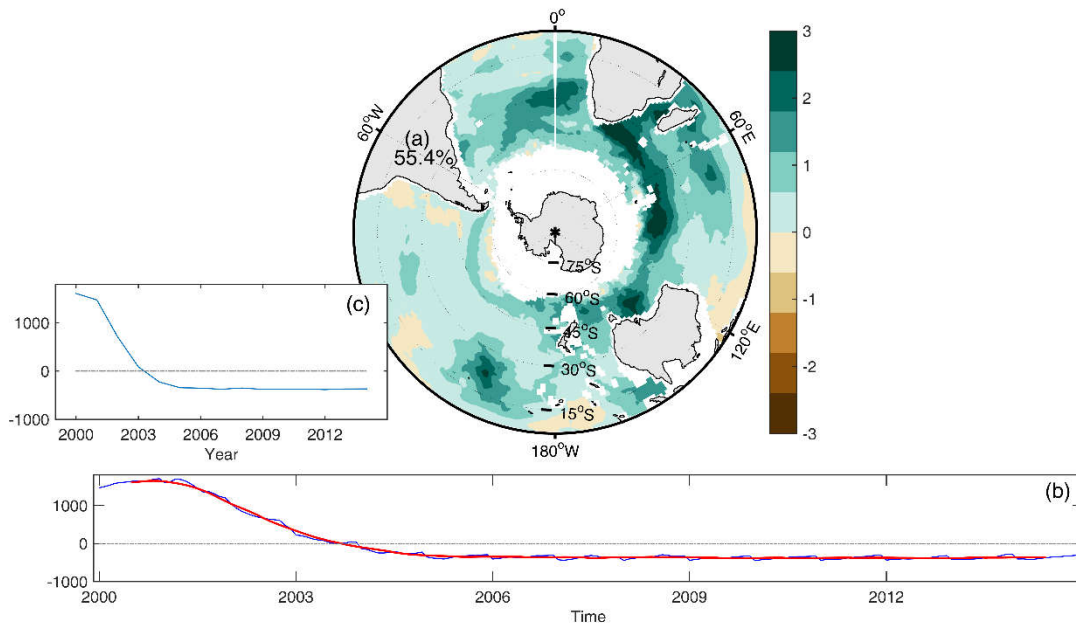
Fig. 8 (a) Pattern and (b) time series (blue: monthly, red: 13-month smooth) of EOF1 of salinity on 27.36$\gamma^n$ surface. (c) Yearly mean time series of EOF1. Calculated from SODA data.

REFERENCES

Beal, L. M., W. P. De Ruijter, A. Biastoch, and R. Zahn (2011), On the role of the Agulhas system in ocean circulation and climate, *Nature.*, *472*(7344), 429-436, doi: 10.1038/nature09983.

Biastoch, A., C. W. Böning, F. U. Schwarzkopf, and J. Lutjeharms (2009), Increase in Agulhas leakage due to poleward shift of Southern Hemisphere westerlies, *Nature.*, *462*(7272), 495-498, doi: 10.1038/nature08519.

Biastoch, A., J. V. Durgadoo, A. K. Morrison, E. van Sebille, W. Weijer, and S. M. Griffies (2015), Atlantic multi-decadal oscillation covaries with Agulhas leakage, *Nature communications*, *6*, doi: 10.1038/ncomms10082.

Bindoff, N. L., and T. J. Mcdougall (1994), Diagnosing climate change and ocean ventilation using hydrographic data, *J. Phys. Oceanogr.*, *24*(6), 1137-1152, doi: 10.1175/1520-0485(1994)024<1137:DCCAOV>2.0.CO;2.

Bindoff, N. L., and T. J. McDougall (2000), Decadal changes along an Indian Ocean section at 32 S and their interpretation, *J. Phys. Oceanogr.*, *30*(6), 1207-1222, doi: http://dx.doi.org/10.1175/1520-0485(2000)030<1207:DCAAIO>2.0.CO;2.

Boebel, O., C. Schmid, and W. Zenk (1997), Flow and recirculation of Antarctic intermediate water across the Rio Grande rise, *J. Geophys. Res. Oceans (1978–2012)*, *102*(C9), 20967-20986, doi: 10.1029/97JC00977.

Carton, J. A., G. A. Chepurin, and L. Chen (2016), An updated reanalysis of ocean climate using the Simple Ocean Data Assimilation version 3 (SODA3), *manuscript in preparation*.

439  Church, J. A., J. S. Godfrey, D. R. Jackett, and T. J. McDougall (1991), A model of sea level
440  rise caused by ocean thermal expansion, *J. Climate.*, *4*(4), 438-456, doi:
441  http://dx.doi.org/10.1175/1520-0442(1991)004<0438:AMOSLR>2.0.CO;2.

442  Close, S. E., A. C. Naveira Garabato, E. L. McDonagh, B. A. King, M. Biuw, and L. Boehme
443  (2013), Control of mode and intermediate water mass properties in Drake Passage by the
444  Amundsen Sea Low, *J. Climate.*, *26*(14), 5102-5123, doi: 10.1175/JCLI-D-12-00346.1.

445  Curry, R., B. Dickson, and I. Yashayaev (2003), A change in the freshwater balance of the
446  Atlantic Ocean over the past four decades, *Nature.*, *426*(6968), 826-829, doi:
447  10.1038/nature02206.

448  De Ruijter, W., A. Biastoch, S. Drijfhout, J. Lutjeharms, R. Matano, T. Pichevin, P. Van
449  Leeuwen, and W. Weiger (1999), Indian-Atlantic interocean exchange: Dynamics, estimation
450  and impact, *J. Geophys. Res.*, *104*(C9), 20885-20910.

451  Donners, J., and S. S. Drijfhout (2004), The Lagrangian view of South Atlantic interocean
452  exchange in a global ocean model compared with inverse model results, *J. Phys. Oceanogr.*,
453  *34*(5),                                    1019-1035,                                    doi:
454  http://dx.doi.org/10.1175/1520-0485(2004)034<1019:TLVOSA>2.0.CO;2.

455  Durgadoo, J. V., B. R. Loveday, C. J. C. Reason, P. Penven, and A. Biastoch (2013), Agulhas
456  Leakage Predominantly Responds to the Southern Hemisphere Westerlies, *J. Phys. Oceanogr.*,
457  *43*(10), 2113-2131, doi: 10.1175/JPO-D-13-047.1.

458  Feely, R. A., R. Wanninkhof, S. Alin, M. Baringer, and J. Bullister (2011), Global Repeat
459  Hydrographic/CO2/Tracer surveys in Support of CLIVAR and Global Cycle objectives:
460  Carbon Inventories and Fluxes.

461  Fetter, A., M. Schodlok, and V. Zlotnicki (2010), Antarctic Intermediate Water Formation in a
462  High-Resolution OGCM, paper presented at EGU General Assembly Conference Abstracts.

463  Goes, M., I. Wainer, and N. Signorelli (2014), Investigation of the causes of historical
464  changes in the subsurface salinity minimum of the South Atlantic, *J. Geophys. Res. Oceans*,
465  *119*(9), 5654-5675, doi: 10.1002/2014JC009812.

466  Gordon, A. L., R. Weiss, W. M. Smethie Jr, and M. J. Warner (1992), Thermociine and
467  Intermediate Water Communication, *J. Geophys. Res.*, *97*(C5), 7223-7240, doi:
468  10.1029/92JC00485.

469  Held, I. M., and B. J. Soden (2006), Robust responses of the hydrological cycle to global
470  warming, *J. Climate.*, *19*(21), 5686-5699, doi: http://dx.doi.org/10.1175/JCLI3990.1.

471  Hosoda, S., T. Ohira, and T. Nakamura (2008), A monthly mean dataset of global oceanic
472  temperature and salinity derived from Argo float observations, *JAMSTEC Rep. Res. Dev.*, *8*,
473  47-59, doi: http://doi.org/10.5918/jamstecr.8.47.

474  Hummels, R., P. Brandt, M. Dengler, J. Fischer, M. Araujo, D. Veleda, and J. V. Durgadoo
475  (2015), Interannual to decadal changes in the western boundary circulation in the Atlantic at
476  11° S, *Geophys. Res. Lett.*, *42*(18), 7615-7622, doi: 10.1002/2015GL065254.

477  Jackett, D. R., and T. J. McDougall (1997), A neutral density variable for the world's oceans, *J.*
478  *Phys.           Oceanogr.*,           *27*(2),           237-263,           doi:
479  http://dx.doi.org/10.1175/1520-0485(1997)027<0237:ANDVFT>2.0.CO;2.

480  Kawano, T., H. Uchida, W. Schneider, Y. Kumamoto, A. Nishina, M. Aoyama, A. Murata, K.
481  Sasaki, Y. Yoshikawa, and S. Watanabe (2004), Cruise Summary of WHP P6, A10, I3 and I4

482    Revisits in 2003, paper presented at AGU Fall Meeting Abstracts.

483    Lübbecke, J. F., J. V. Durgadoo, and A. Biastoch (2015), Contribution of increased Agulhas

484    leakage to tropical Atlantic warming, *J. Climate.*, *28*(24), 9697-9706, doi:

485    http://dx.doi.org/10.1175/JCLI-D-15-0258.1.

486    Le Bars, D., J. V. Durgadoo, H. A. Dijkstra, A. Biastoch, and W. P. M. De Ruijter (2014), An

487    observed 20-year time series of Agulhas leakage, *Ocean. Sci.*, *10*(4), 601-609, doi:

488    10.5194/os-10-601-2014.

489    Lee, S. K., W. Park, E. van Sebille, M. O. Baringer, C. Wang, D. B. Enfield, S. G. Yeager, and

490    B. P. Kirtman (2011), What caused the significant increase in Atlantic Ocean heat content

491    since the mid‐20th century?, *Geophys. Res. Lett.*, *38*(17), doi: 10.1029/2011GL048856.

492    Loveday, B., P. Penven, and C. Reason (2015), Southern Annular Mode and westerly‐

493    wind‐driven changes in Indian‐Atlantic exchange mechanisms, *Geophys. Res. Lett.*, *42*(12),

494    4912-4921, doi: 10.1002/2015GL064256.

495    McCarthy, G., E. McDonagh, and B. King (2011), Decadal variability of thermocline and

496    intermediate waters at 24 S in the South Atlantic, *J. Phys. Oceanogr.*, *41*(1), 157-165, doi:

497    10.1175/2010JPO4467.1.

498    McCarthy, G. D., B. A. King, P. Cipollini, E. L. McDonagh, J. R. Blundell, and A. Biastoch

499    (2012), On the sub-decadal variability of South Atlantic Antarctic Intermediate Water,

500    *Geophys. Res. Lett.*, *39*, L10605, doi: 10.1029/2012GL051270.

501    McCartney, M. S. (1977), Subantarctic Mode Water, in *Angel, M.V. (Ed.), A Voyage of*

502    *Discovery: George Deacon 70th Anniversary Volume (Suppl. To Deep-Sea Res.). Pergamon*,

503    edited, pp. 103-119, Woods Hole Oceanographic Institution.

504    McCartney, M. S. (1982), The subtropical recirculation of mode waters, *J. Mar. Res.*, *40*,

505    427-464.

506    McDougall, T. J. (1987), Neutral surfaces, *J. Phys. Oceanogr.*, *17*(11), 1950-1964, doi:

507    http://dx.doi.org/10.1175/1520-0485(1987)017<1950:NS>2.0.CO;2.

508    Naveira Garabato, A. C., L. Jullion, D. P. Stevens, K. J. Heywood, and B. A. King (2009),

509    Variability of Subantarctic Mode Water and Antarctic Intermediate Water in the Drake

510    Passage during the Late-Twentieth and Early-Twenty-First Centuries, *J. Climate.*, *22*(13),

511    3661-3688, doi: 10.1175/2009jcli2621.1.

512    Orsi, A. H., T. Whitworth Iii, and W. D. Nowlin Jr (1995), On the meridional extent and fronts

513    of the Antarctic Circumpolar Current, *Deep-Sea Res. I.*, *42*(5), 641-673, doi:

514    http://dx.doi.org/10.1016/0967-0637(95)00021-W.

515    Piola, A. R., and D. T. Georgi (1982), Circumpolar properties of Antarctic intermediate water

516    and Subantarctic Mode Water, *Deep-Sea Res. A.*, *29*(6), 687-711, doi:

517    10.1016/0198-0149(82)90002-4.

518    Ridgway, K. R., and J. R. Dunn (2007), Observational evidence for a Southern Hemisphere

519    oceanic supergyre, *Geophys. Res. Lett.*, *34*, L13612, doi: 10.1029/2007gl030392.

520    Roemmich, D., J. Church, J. Gilson, D. Monselesan, P. Sutton, and S. Wijffels (2015),

521    Unabated planetary warming and its ocean structure since 2006, *Nature Clim. Change*, *5*(3),

522    240-245, doi: 10.1038/nclimate2513.

523    Santoso, A., and M. H. England (2004), Antarctic Intermediate Water circulation and

524    variability in a coupled climate model, *J. Phys. Oceanogr.*, *34*(10), 2160-2179, doi:

http://dx.doi.org/10.1175/1520-0485(2004)034<2160:AIWCAV>2.0.CO;2.

Schmidtko, S., and G. C. Johnson (2012), Multidecadal Warming and Shoaling of Antarctic Intermediate Water*, *J. Climate.*, *25*(1), 207-221, doi: 10.1175/jcli-d-11-00021.1.

Skliris, N., R. Marsh, S. A. Josey, S. A. Good, C. Liu, and R. P. Allan (2014), Salinity changes in the World Ocean since 1950 in relation to changing surface freshwater fluxes, *Climate dynamics*, *43*(3-4), 709-736, doi: 10.1007/s00382-014-2131-7.

Sloyan, B. M., and S. R. Rintoul (2001), Circulation, Renewal, and Modification of Antarctic Mode and Intermediate Water*, *J. Phys. Oceanogr.*, *31*(4), 1005-1030, doi: http://dx.doi.org/10.1175/1520-0485(2001)031<1005:CRAMOA>2.0.CO;2.

Speich, S., B. Blanke, and W. Cai (2007), Atlantic meridional overturning circulation and the Southern Hemisphere supergyre, *Geophys. Res. Lett.*, *34*, L23614, doi: 10.1029/2007GL031583.

Speich, S., B. Blanke, P. de Vries, S. Drijfhout, K. Döös, A. Ganachaud, and R. Marsh (2002), Tasman leakage: A new route in the global ocean conveyor belt, *Geophys. Res. Lett.*, *29*(10), 1416, doi: 10.1029/2001gl014586.

Sun, C., and D. R. Watts (2002), A view of ACC fronts in streamfunction space, *Deep-Sea Res. I.*, *49*(7), 1141-1164, doi: 10.1016/S0967-0637(02)00027-4.

Sverdrup, H. U., M. W. Johnson, and R. H. Fleming (1942), *The Oceans: Their physics, chemistry, and general biology*, Prentice-Hall New York.

Swart, N., and J. Fyfe (2012), Observed and simulated changes in the Southern Hemisphere surface westerly wind ‐ stress, *Geophys. Res. Lett.*, *39*(L16711), doi: 10.1029/2012GL052810.

Talley, L. D. (1996), Antarctic intermediate water in the South Atlantic, in *The South Atlantic: Present and Past Circulation*, edited, pp. 219-238, Springer.

Talley, L. D. (2013), Closure of the global overturning circulation through the Indian, Pacific, and Southern Oceans: Schematics and transports, *Oceanography*, *26*(1), 80-97, doi: http://dx.doi.org/10.5670/oceanog.2013.07.

Trenberth, K. E., W. G. Large, and J. G. Olson (1989), The effective drag coefficient for evaluating wind stress over the oceans, *J. Climate.*, *2*(12), 1507-1516, doi: http://dx.doi.org/10.1175/1520-0442(1989)002<1507:TEDCFE>2.0.CO;2.

van Sebille, E., A. Biastoch, P. Van Leeuwen, and W. De Ruijter (2009), A weaker Agulhas Current leads to more Agulhas leakage, *Geophys. Res. Lett.*, *36*(3), doi: 10.1029/2008GL036614.

Wong, A. P., N. L. Bindoff, and J. A. Church (1999), Large-scale freshening of intermediate waters in the Pacific and Indian Oceans, *Nature.*, *400*(6743), 440-443, doi: 10.1038/22733.

Wong, A. P., N. L. Bindoff, and J. A. Church (2001), Freshwater and heat changes in the North and South Pacific Oceans between the 1960s and 1985-94, *J. Climate.*, *14*(7), 1613-1633, doi: http://dx.doi.org/10.1175/1520-0442(2001)014<1613:FAHCIT>2.0.CO;2.